ELSEVIER

Journal of Hydrology 265 (2002) 195–211

Journal of Hydrology

www.elsevier.com/locate/jhydrol

Apparent translatory flow in groundwater recharge and runoff generation

Gunnar Lischeid[a,*], Andreas Kolb[a,1], Christine Alewell[b,1]

[a]*Department of Hydrogeology, BITÖK, University of Bayreuth, Dr-Hans-Frisch-Straße 1-3, D-95440 Bayreuth, Germany*
[b]*Department of Soil Ecology, BITÖK, University of Bayreuth, Dr-Hans-Frisch-Straße 1-3, D-95440 Bayreuth, Germany*

Received 31 October 2001; revised 11 April 2002; accepted 3 May 2002

Abstract

A sound understanding of solute transport under stormflow conditions is crucial for assessing groundwater and stream water contamination risk. The vadoze zone exhibits its maximum protective effect, when solute transport occurs via translatory flow. In contrast, short-term hydraulic short circuits via preferential flow can have considerable harmful effects on water quality.

The Lehstenbach study combines comprehensive physical and hydrochemical measurements that allow improved understanding of the short-term stream discharge and groundwater recharge dynamics. The data set covers the 1998 catchment wetting-up period, including the second to highest discharge peak, since measurements began in 1987. During that storm, the pressure wave reached 0.9 m depth within 2 h, preceding the discharge peak by another 2 h. In contrast, shallow groundwater response at 3 m depth was delayed considerably.

Soil hydrometric data and temperature, aluminum, sulfate, and dissolved organic carbon dynamics in stream water and groundwater indicated translatory flow during groundwater recharge and stormflow runoff generation. In contrast, the observed decline in silica concentration of groundwater and stream water provided strong evidence that seepage flux was restricted to a small fraction of the total soil water pool. Exchange with the matrix was limited by the slow kinetics of silica dissolution, while sulfate and aluminum kinetics are quite rapid, and this feature explains the apparent discrepancy between silica, sulfate, and aluminum data.

The results emphasize that preferential flow phenomena are not so much due to inherent properties of the soil matrix as depending on the scale of observation and the observed parameters and their kinetics of equilibrating with the matrix during subsurface transport.

Keywords: Groundwater recharge; Runoff generation; Preferential flow; Kinetics; Ion exchange; Sulfate; Aluminum; Silica; Lehstenbach catchment

1. Introduction

Preferential flow processes are of major concern to hydrologists and biogeochemists. Many studies have shown that quickly infiltrating contaminated water that bypasses the soil matrix and its buffering potential as preferential flow is a major threat to groundwater (Zoller et al., 1998; Landon et al., 2000) and stream water (Kirkby, 1988; Goodrich and Woolisher, 1991; Bonell, 1998) quality.

However, different definitions of preferential flow

* Corresponding author. Fax: +49-921-555-799.
E-mail addresses: gunnar.lischeid@bitoek.uni.bayreuth.de (G. Lischeid), andreas.kolb@bitoek.uni.bayreuth.de (A. Kolb), christine.alewell@bitoek.uni.bayreuth.de (C. Alewell).
[1] Fax: +49-921-555-799.

0022-1694/02/$ - see front matter
PII: S0022-1694(02)00108-7

exist. One common definition is based on pore space geometry. Preferential flow is ascribed to water transport in pores that exceed a certain diameter, which are called macropores (Leaney et al., 1993; Noguchi et al., 1999). However, different authors cite different threshold values for the effective pore diameter (Beven and German, 1982; Luxmoore et al., 1990). In addition, the connectivity of the macropores plays an important role that is difficult to quantify at larger scales (Beven and German, 1982).

Other authors define preferential flow as the fraction of water and solute transport that occurs decoupled from the soil matrix, i.e. soil matrix potential (non-Darcian flow; e.g. Göttlein and Manderscheid (1998) and Beven and German (1982)) or solute concentration (Stewart and McDonnell, 1991; Leaney et al., 1993). Quantification of preferential flow then depends on the observed parameters and the scale of observation. Many studies used tracers to distinguish between event water and pre-event water. Event water is defined to be the portion of rainfall that reaches the stream or the groundwater during the specific rainstorm, which is often ascribed to preferential flow (Beven and German, 1982; Jones, 1987; Bonell, 1998).

'Translatory flow' describes piston-flow displacement of pre-event water from the soil pore space due to the increasing pressure of infiltrating new water (Anderson et al., 1997; Rawlins et al., 1997; McDonnell, 1990). When the effective porosity of the soil is minimal, the speed of the subsurface pressure wave might be of the same order of magnitude as that of surface runoff and could explain the oft-observed rapid stream hydrograph responses and the dominance of pre-event water in stormflow of low order watersheds (Kirkby, 1988; Bonell, 1998; Anderson et al., 1997).

Due to the dependence of subsurface water flow on pore diameter as described by the Hagen–Poiseuille equation, every flow in natural porous media is preferential flow at the micro scale. However, the translatory flow concept can be a useful approximation for describing subsurface transport at larger scales. It has to be kept in mind that preferential flow phenomena are not so much due to inherent properties of the soil matrix as depending on the scale of observation and the observed parameters (e.g. tracer concentration) and their kinetics of equilibrating with the matrix during subsurface transport. Preferential flow is then more likely for substances that react very slowly with the matrix or even not at all, e.g. ^{2}H and ^{18}O isotopes, whereas preferential flow is often unlikely with ions that are quickly exchanged with the soil exchange complex (Robson et al., 1993). This is addressed, e.g. by the two regions approach, which assumes kinetically constrained exchange between the mobile and the immobile fraction of the soil water pool (Gerke and van Genuchten, 1993; Flühler et al., 1996).

Conservative mixing of event water and pre-event water can result in stream water solute concentrations very similar to those of the pre-event soil water, since the amount of infiltrating rain or melt water is usually very small compared to the soil's or aquifer's total water storage (Waddington et al., 1993; Brassard et al., 2000; Landon et al., 2000).

Knowledge of these processes and their adequate implementation in models is crucial to water quality risk assessment. For example, Beven (2001a) points out that quick return flow is often modeled as purely surface flow, which does not have implications for modeling of the hydrograph, but for stream water chemistry modeling. Thus, different authors emphasize the value of field data that are still not adequately addressed by hydrological models (Beven, 2001b; Rice and Hornberger, 1998; Bonell, 1998).

The study presented here is part of a large project designed to investigate the impact of acid deposition on soil and water quality in forested areas (Sager et al., 1990; Matzner et al., 2001). In 1987, a comprehensive hydrological monitoring program was instituted at the Lehstenbach catchment in southern Germany. The catchment is well suited to the study of groundwater recharge and stormflow generation processes, because the surface is not sealed, and impeding layers in the soil are restricted to small areas. The aquifer is some tens of meters thick, thus the bedrock surface topography does not play an important role in groundwater flow, unlike many intensively studied small order catchments (cf. Burns et al., 1998).

The aim of the study is to investigate the extent to which water flow and solute transport during groundwater recharge and stormflow discharge can be described as translatory flow, preferential flow, or complete mixing with respect to soil hydrometric data and various solutes that differ in their reactivity with

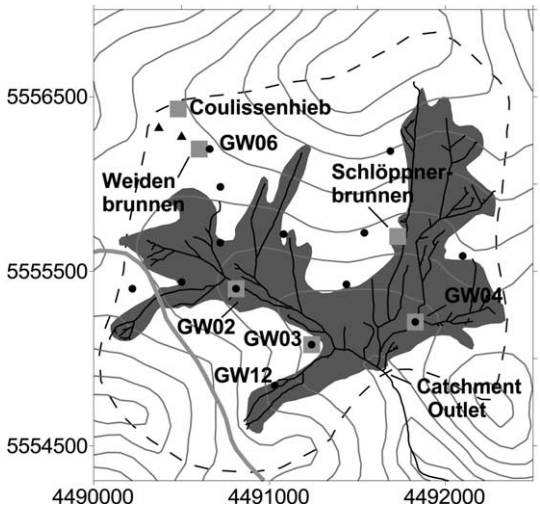

Fig. 1. Map of the Lehstenbach watershed. The hatched area denotes wetland soils (fens and bogs) according to the forestry administration soil map. Solid circles: groundwater wells; gray squares: integrated sites; triangles: detailed meteorological measurements; thin gray lines: contour levels at 20 m intervals; thick gray line: public road. Gauss-Krüger coordinates at the *x*- and *y*-axes are given in m; *y*-axis in north–south direction.

the soil matrix. It is intended to provide a basis for better understanding and modeling of solute turnover at the watershed scale.

2. Site description

The study took place in the Lehstenbach watershed (50°08′N and 11°52′E) in the Fichtelgebirge mountains in southeast Germany. Watershed area is about 4.2 km^2 and elevation ranges from 695 to 877 m amsl. The bedrock is variscan granite. Bedrock outcrops exist only at the mountaintop in the southwestern part of the watershed (Fig. 1) and the regolith is up to 40 m thick due to intensive tertiary weathering. The region was not glaciated during the last ice age. The regolith consists of a heterogeneous interlayering of loamy sand, grus, and massive boulders up to several meters in diameter. Dystric cambisols and podzols predominate. In the riparian zone, fibric histosols and dystric gleysols are abundant, comprising 35% of the watershed area. Poorly permeable layers are found at the base of soliflucted till deposits.

Land use is exclusively forest with Norway spruce covering more than 95% of the watershed area. Closed-canopy forest is dominant, even on the wetland soils. The climate is humid continental. Annual mean air temperature is about 5–6.5 °C, depending on altitude. In the 1988–1999 period, annual mean precipitation was 985 mm. Mean runoff was 461 mm, yielding a runoff coefficient of 0.47. Snowpack usually develops in January and persists until March.

Mean groundwater level is more than 10 m below the surface in the upper parts of the watershed, and close to the surface in one third of the watershed area. Groundwater flow in the fractured bedrock is assumed to be negligible compared to flow in the overlying regolith (Lange et al., 1995). Saturated hydraulic conductivity is roughly 10^{-4} m s^{-1} in the top soil (Moritz et al., 1994), and 3×10^{-6} m s^{-1} in the aquifer (Hauck, 1999). There is no evidence of a macropore system that could contribute considerable amounts of water to stream discharge during rainstorms. The effective porosity of the aquifer is about 10% (Hauck, 1999).

The watershed is drained by a dense network of natural streams and artificial channels, part of which are ephemeral, especially at higher altitudes. According to the 1:25,000 topographic map, the stream net density is 2.4 km km^{-2}. Groundwater gradients and subsequent discharge measurements along the streams indicate that the streams are gaining throughout their courses. Flow velocity in the main tributaries was determined under baseflow conditions, being between 600 and 3000 m h^{-1}. Thus, it is assumed that the mean time delay due to channel routing within the watershed is less than 1 h under storm conditions. In addition, most of the contributing area is likely to be close to the catchment runoff. Thus, time delay due to channel routing is not considered in this study.

The catchment outlet is located in a small incision in the southeastern edge of the bowl-shaped watershed (Fig. 1). Groundwater flow in the regolith parallel to the stream at the catchment outlet is likely to comprise only a negligible portion of the total outflow.

3. Measurements

Meteorological parameters including precipitation,

air temperature, etc. are measured continuously from a 30 m tower at the Weidenbrunnen site, and at a clearing about 275 m west of the tower, both roughly at 765 m amsl (Fig. 1). Time resolution is 10 min throughout the year. In an earlier study, open field precipitation was measured at sites at 705, 770, and 785 m amsl (Moritz et al., 1994). No significant differences were found.

Several 'integrated' sites that cover a wide range of tree age, mean groundwater level and distance from the next stream were instrumented. In 1998, throughfall (amount and solute concentration) was collected at four of these sites by 15 (Weidenbrunnen, GW02, GW03) and 20 (Coulissenhieb) samplers per site at biweekly intervals, yielding 29 aggregated samples per date in total. Suction cups at 0.2, 0.5, 0.9, and 1.0 m depth collected soil solution at biweekly intervals. The vacuum was maintained between −200 and −300 hPa. In total, 59 suction cups were probed on each sampling day in 1998.

Soil matrix potential, soil water content, and soil temperature were measured at six sites at up to 0.9 m in depth at hourly intervals. A plastic frill at the soil surface prevented water from pouring down the tensiometer shafts. Prior studies confirmed that horizontally and vertically installed tensiometers do not differ with respect to response time or magnitude of readings. In the wetland areas, tensiometers and TDR probes were installed on top of the small hummocks on the softly undulating surface. TDR probes were installed at a 45° angle from the surface. Soil temperature was measured close to the pressure transducer of the tensiometers, about 10 cm from the lower end of the tensiometer. Up to 20 tensiometers per depth had been installed at the Coulissenhieb, Weidenbrunnen and Schlöppnerbrunnen sites in the first years of the study (1993–1995). The number of replicates per site was reduced in 1996 due to the very similar observations, especially during the wet season. This allowed to monitor additional sites.

Groundwater level was measured at monthly intervals, and groundwater solute concentrations at bimonthly intervals in 13 wells. Depth integrated samples were taken by a submerged pump. In addition, groundwater level, temperature, and hydrochemical parameters were recorded at hourly intervals in wells GW03 and GW12 (Fig. 1). Well GW03 is screened from 2 to 8 m and from 9 to 15.4 m below the surface, and the probe was installed 4.4 m below the surface. The drilling core reveals two sandy layers at 0–5 and 10–10.5 m below the surface. Granite, at varying stages of weathering, was found between 5–10 and 10.5–16 m below the surface. Rötting (2000) showed that 20% of the total inflow into GW03 occurred rather homogeneously in the upper 2–9 m depth interval, and the remaining 80% flowed in from the 9 to 12 m depth interval.

GW12 is screened between 7 and 10 m below the surface, and the probe was installed at 7.2 m below the surface. Here, two clay layers exist at 1.2–1.8 and 2.2–4.0 m depth. However, sandy layers prevail in the drilling core. Below 5.8 m, granite boulders comprise a substantial part of the matrix. Well GW06 is located about 100 m from the Weidenbrunnen site. Down to 16 m, sandy layers prevail. At 1.5–2.5, 5.25–7, and 10–11.5 m the drilling core contains granite rock. At all wells, a concrete slab of about 1 m^2 protects the wellhead. In addition, clay pellets to 2 m depth seal the pipe.

Depth specific groundwater sampling was performed at six wells in 4–20 m depth. There were no significant correlations of sulfate, aluminum, silica or dissolved organic carbon (DOC) concentration with depth for the pooled data from all wells. This does not hold for single wells. The median of solute concentration decrease with depth is 0.0002 mmol l^{-1} m^{-1} for sulfate, 0.003 mmol l^{-1} m^{-1} for aluminum, and 0.0014 mmol l^{-1} m^{-1} for DOC. In contrast, silica concentration increases with depth with a median gradient of 0.004 mmol l^{-1} m^{-1} (Rötting 2000).

Stream discharge and stream water solute concentrations were measured at the catchment outlet. Grab samples were taken biweekly. An autosampler took samples at hourly intervals, which were then mixed in equal ratios to yield a daily composite. Discharge was also measured at 1 h intervals.

Water samples were stored in the dark at less than 4 °C. They were filtered through a cellulose-membrane filter with 0.45 μm pore size. Sulfate concentration was determined by ion exchange chromatography (Dionex 200i-SP). Silica and aluminum concentration were measured by atomic emission spectrometry with inductively coupled plasma (Integra XMP, GBC). Concentration of DOC was determined as CO_2 by infrared detection after persulfate-UV-oxidation (Foss Heraeus LiquiTOC).

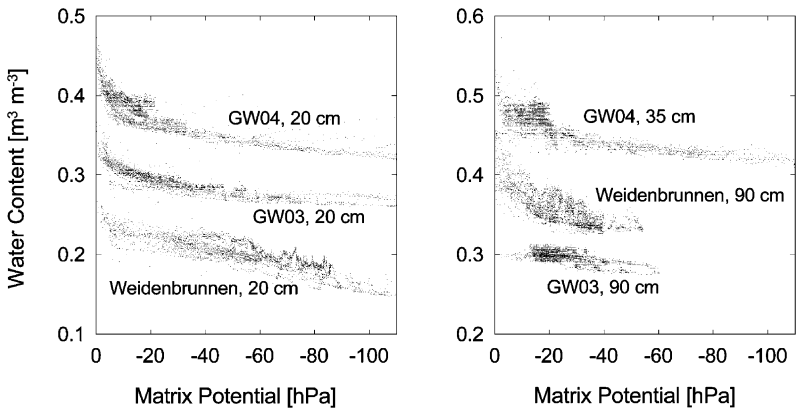

Fig. 2. Water retention relationship, determined by adjacent tensiometers and TDR probes at different sites in the Lehstenbach watershed.

4. Results

4.1. Water capacity of the vadoze zone

The lower the effective porosity of the matrix, the faster a pressure wave can propagate through the soil. However, the relationship between soil water content and soil matrix potential must be known in order to investigate this effect. Data from 13 TDR probe and tensiometer pairs from July 1 to December 31, 1998 period were used to derive field relationships (Fig. 2). Data scattering is ascribed to both the limited accuracy of the TDR readings (about 0.01 $m^3\ m^{-3}$), and to small-scale heterogeneities. Spacing between TDR probes and tensiometers at the same depth was less than 1 m. Due to high precipitation amounts, matrix potential less than -200 hPa was only rarely observed in 1998. This might be a reason why hysteresis between water content and matrix potential was not very pronounced.

The median of soil water content data for the ranges $[-1; 0]$, $[-11; -10]$, and $[-105; -95]$ hPa was calculated for each TDR and tensiometer pair to quantify soil water capacity. The resulting roughly 5% increase of volumetric water content in the range of -10–0 hPa is about the same as that for the -100 to -10 hPa range (Table 1).

Table 1
Water capacity (change of volumetric water content within different ranges of matrix potential) determined by adjacent tensiometers and TDR probes in the Lehstenbach topsoil

	$[-10; 0]$ hPa (%)	$[-100; -10]$ hPa (%)
Median	5.1	6.2
1. Quartile	3.2	3.4
3. Quartile	5.7	9.9

4.2. Topography of the riparian zone

The soil surface was investigated in detail at site GW02, where the slope is rather homogeneously directed east to an area of about $85 \times 75\ m^2$ in order to better understand runoff generation in the riparian zone. The surface was leveled at 83 points. Subtracting the general decline (linear regression of all levels) from the local elevation yielded residuals with a Gaussian distribution (Kolmogorov–Smirnov test with Lilliefors correction, 0.05 level of significance) with a standard deviation of 0.347 m. Thus, 2.5% of the area is saturated to the surface, when the mean groundwater level is 0.68 m below mean surface, and 10% when the mean groundwater level is 0.445 m below mean surface.

The correlation length is less than the mean spacing of survey points (9 m). Visual inspection revealed that the hollows form irregular patches rather than interconnected rivulets. Nevertheless, it was observed that surface water flow in the hollows exhibited quite high flow velocities during rainstorms. This was obviously due to subsurface flow between single patches within or underneath the litter layer.

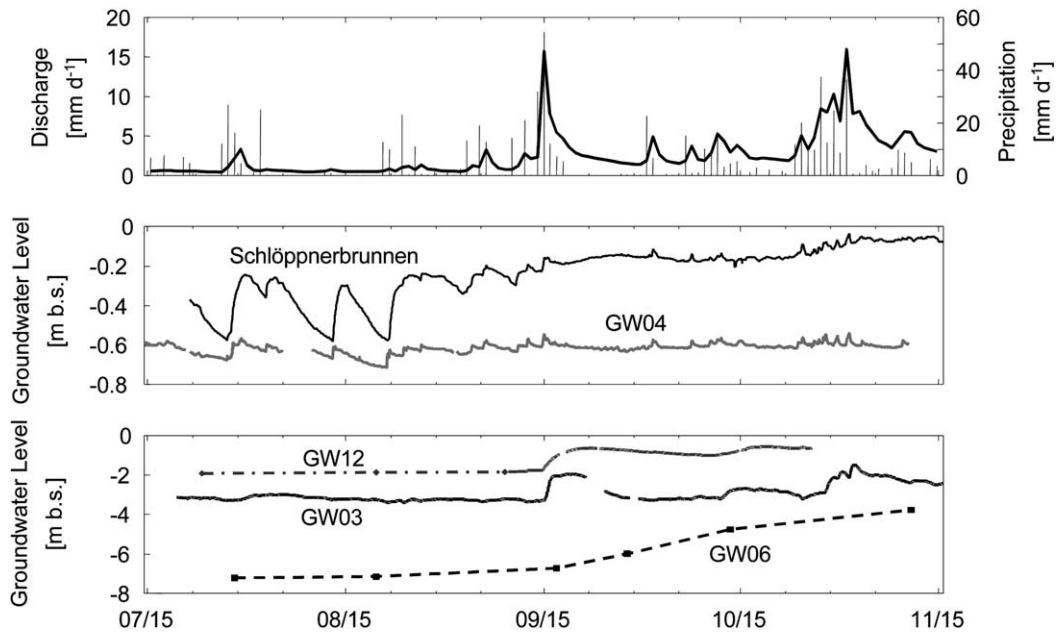

Fig. 3. Time series of stream discharge, precipitation and groundwater levels at various sites in fall 1998.

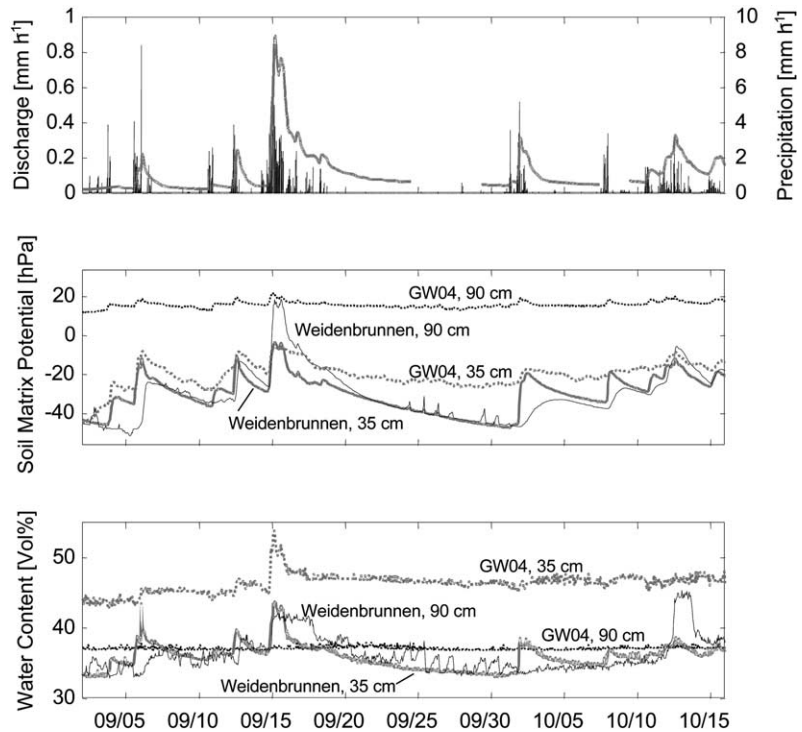

Fig. 4. Time series of precipitation, discharge at the catchment outlet (upper panel), matrix potential (middle panel), and soil water content (lower panel) at different sites in fall 1998.

Table 2
Mean lag time between maximum rainfall intensity, and maximum soil matrix potential and peak discharge on September 15. The number of replicates is given in brackets

Parameter	Depth (m)	Median (h)	Range (h)
Soil matrix potential	0.20	0 (9)	0–0
Soil matrix potential	0.35	0.5 (10)	0–2
Soil matrix potential	0.90	2 (9)	0–6
Groundwater level (GW03)	3.28–2.10	32 (1)	–
Groundwater level (GW12)	1.64–0.63	175 (1)	–
Runoff	–	4 (1)	–

4.3. Hydrometric data

In July and August 1998, catchment discharge was fairly constant and only occasionally exceeded 0.5 mm day^{-1} (Fig. 3) and groundwater levels at greater depths (>1 m below surface) did not change before mid-September. In contrast, the shallow groundwater level at GW04 clearly reacts even during minor rainstorms. The amplitude of groundwater level fluctuations was less than 0.2 m. At the more up-hill Schlöppnerbrunnen site, groundwater level increased by up to 0.4 m during single rainstorms and decreased again thereafter, until the end of August.

A series of rainstorms occurred at the end of August. From September 1 to October 20, precipitation was 300 mm. The highest intensity of 74 mm day^{-1} occurred between 18:00 on September 14 and 18:00 on September 15. Another 55 mm of precipitation was recorded between October 10 and 18.

The September 15 discharge peak of 1039 l s^{-1} (0.89 mm h^{-1}) was the second to highest observed in the watershed since the end of 1986 (Fig. 3). Discharge increased by a factor of 20 within 21 h. The runoff coefficient (ratio of runoff over precipitation) between September 12 and 23 was 0.40. Subtracting the base flow of about 24 l s^{-1} or 0.02 mm h^{-1} observed prior to the rainstorm, the runoff coefficient was 0.35, which is equal to the portion of wetland soils of the watershed area (Fig. 1).

As a consequence, the hydrological behavior of the catchment changed considerably. Discharge did not fall below 1 mm day^{-1} until the end of 1998 (Fig. 3). In contrast to the preceding period, groundwater level at the Schlöppnerbrunnen site remained close to the surface, and the range of fluctuations was very similar to that at the GW04 site from that point forward. Similarly, even at up-slope sites where the depth to the water table exceeded several meters, the groundwater level started to increase (Fig. 3).

In general, matrix potential in the top soil (0.2 m depth) exceeded −100 hPa at most sites prior to September 15, indicating that preceding rainstorms almost completely rewetted the top soil after the end of the vegetation growth period. Time series of matrix

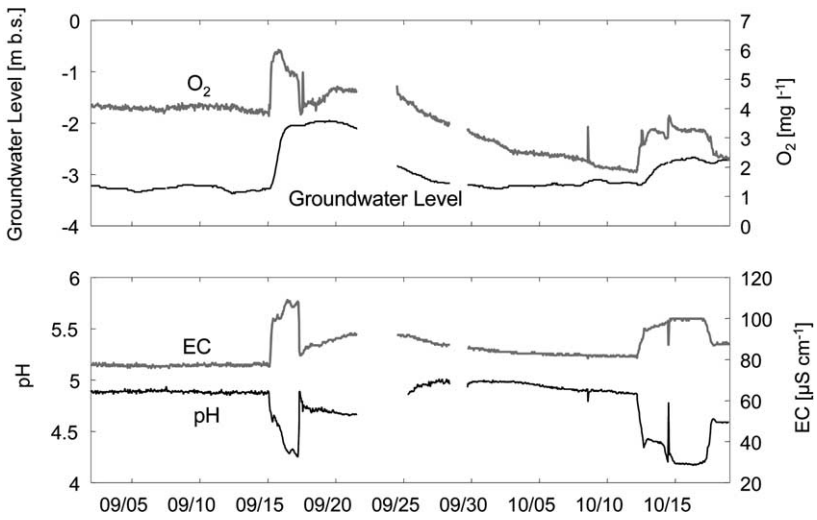

Fig. 5. Groundwater level, oxygen concentration (upper panel), pH and electrical conductivity (lower panel) at well GW03 in fall 1998. The sharp peaks of pH and electrical conductivity on October 14 are artifacts of groundwater sampling.

Table 3
Delay between maximum of rainfall intensity and maximum discharge, calculated based on hourly values June 1–November 30, 1998

Delay (h)	2	3	4	5
Number of cases	13	16	12	3

potential at various sites differ with respect to level and amplitude. At all sites, soil matrix potential increased within a few hours on September 15 (Fig. 4). The increase was much less at sites, where matrix potential indicated saturation prior to the September 15 rainstorm. For example, at GW04, located in the riparian zone close to the stream (Fig. 1), the increase of soil matrix potential at 90 cm depth was less than 10 hPa. This is less than half the groundwater level increase required to store 74 mm of precipitation (see above) in soil with a total porosity of 37% (indicated by TDR measurements), thus strongly suggesting rapid lateral flow of excess water.

The shape of the matrix potential curves was very similar to the hydrograph. Even minor peaks of rainfall intensity were reflected by soil matrix potential data and discharge (Fig. 4). Time series of soil water content paralleled soil matrix potential in the unsaturated zone, and remained constant during saturation.

Mean lag time between rainfall intensity and discharge was 4 h, while it was less than 1 h for soil matrix potential at 0.20 and 0.35 m depth (Table 2). Only at 0.90 m depth did soil matrix potential in the wetland sites react more rapidly than in the remaining three sites. The speed of the pressure wave was about 0.70 m h^{-1} from the soil surface to 35 cm depth, 0.36 m h^{-1} for 35–90 cm depth, and roughly 0.08 m h^{-1} for the 90–328 cm depth interval at GW03 (Table 2, Fig. 4).

Groundwater level at GW03 began to rise 24 h after the 5:00 onset of the September 14 rainstorm, and 3 h after the rainstorm peak at 2:00 on September 15. It reached a first plateau 29 h later, and began to fall 4 days after the plateau (Fig. 5). At well GW12, the maximum groundwater level was observed 1 week after the rainstorm. Due to coarser temporal resolution data, groundwater level increase at GW06 cannot be attributed to single rainstorms (Fig. 3).

In addition, the time delay between peak rainfall and peak discharge was investigated based on hourly values for the June 1–November 30 period. Snowpack did not develop before the beginning of December. In 44 cases, maximum rainfall intensity was at least 0.5 mm h^{-1}, and the increase of discharge at least 1.0 l s^{-1} or 0.0009 mm h^{-1}, respectively. The time delay was between 2 and 5 h (Table 3). Time delay is not correlated with rainfall intensity, discharge, or increase of discharge. Instead, the ratio between peak discharge and maximum rainfall intensity increases significantly (Spearman rank correlation, $p < 0.001$) starting in September, corresponding to increasing soil rewetting and increasing groundwater level (Fig. 3). Again, this ratio is not correlated with maximum rainfall intensity.

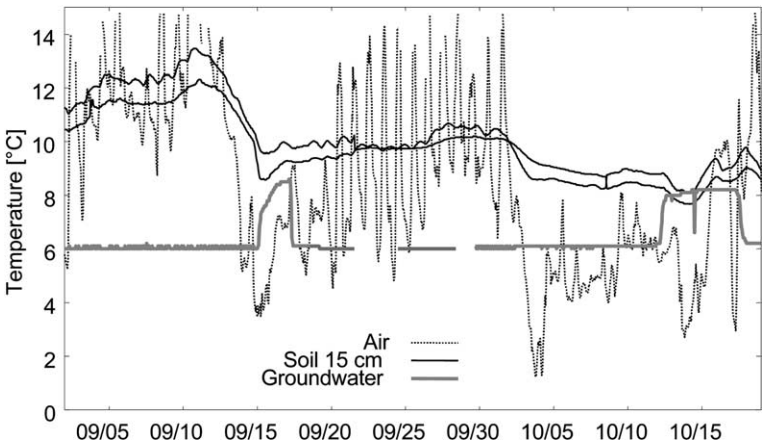

Fig. 6. Temperature in air, soil (two sensors at 15 cm depth at site GW03) and groundwater (site GW03) in fall 1998. The sharp decrease of groundwater temperature on October 14 is an artifact of groundwater sampling.

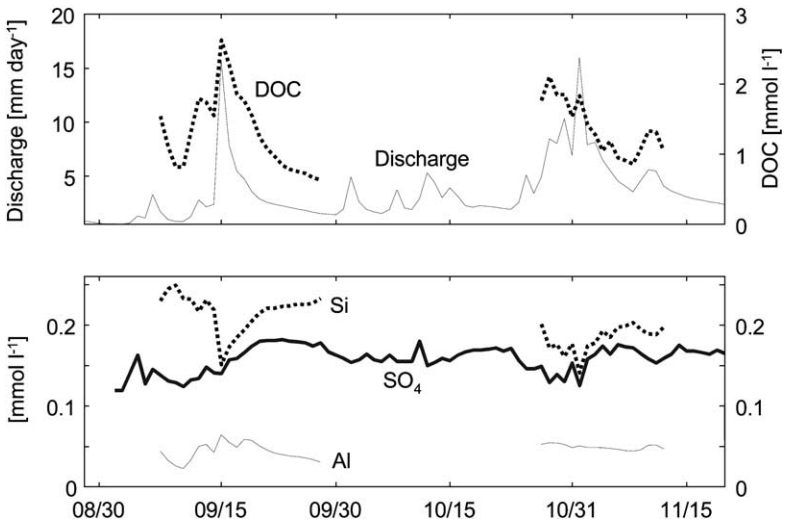

Fig. 7. Time series of discharge and solute concentration in catchment runoff.

4.4. Temperature data

Air temperature decreased by 10 °C within 3 days and was less than 4 °C on September 15 (Fig. 6). Soil temperature at 15 cm depth was considerably more damped and delayed than air temperature. In contrast, groundwater temperature at 4.4 m depth increased to more than 8 °C until September 18. A similar increase of groundwater temperature despite lower air temperature was observed 1 month later at the same site (Fig. 6).

4.5. Solute concentration

DOC concentration in catchment runoff increased and silica decreased with discharge in the short-term (Fig. 7). Aluminum concentration increased with discharge in mid-September, but remained fairly constant at a rather high level in the end of October. In contrast, sulfate concentration decreased only slightly during the major discharge peaks, but clearly increased after the mid-September discharge peak.

Groundwater samples were taken by depth-integrating sampling. At GW03, sulfate and aluminum exhibited an increase, and silica a decrease after mid-September (Fig. 8). DOC concentration was below the detection limit of 0.167 mmol l^{-1}.

Table 4 gives the range of solute concentrations in throughfall and soil solution (0.2–1.0 m depth) measured at four different sites during the second half of 1998. Soil solution data do not show any clear trend for this time period. High solute concentrations in throughfall were only observed in dry periods with very low precipitation amounts. For the remaining

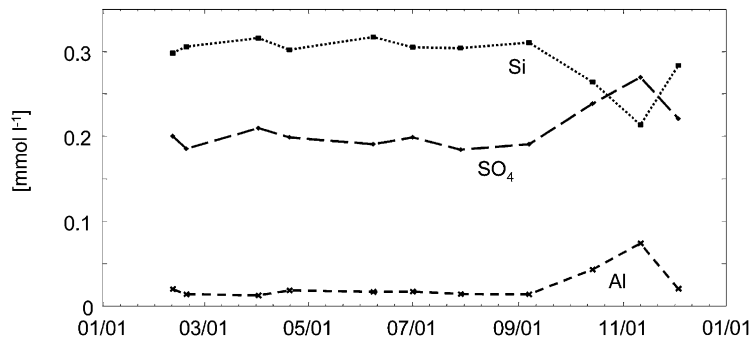

Fig. 8. Time series of solute concentration in groundwater at GW03 (depth integrated sampling).

Table 4
Median and range of solute concentration in throughfall and soil solution (0.2–1.0 m) measured at four different sites in the Lehstenbach watershed July–December 1998

	pH	El. Cond. ($\mu S\ cm^{-1}$)	SO_4 ($mmol\ l^{-1}$)	Al ($mmol\ l^{-1}$)	Si ($mmol\ l^{-1}$)	DOC ($mmol\ l^{-1}$)
Throughfall						
Minimum	3.04	10	0.012	<0.007	<0.007	0.220
Median	4.27	37	0.034	<0.007	<0.007	1.017
Maximum	6.86	565	0.370	0.010	0.020	5.070
Soil solution						
Minimum	2.82	21	0.007	<0.007	0.070	0.210
Median	4.06	96	0.162	0.157	0.213	0.403
Maximum	6.17	314	0.800	0.745	0.480	8.150

sampling dates, maximum throughfall concentrations of sulfate, aluminum, and silica were far below those of stream water and groundwater. In general, the higher the stream discharge or groundwater level, the more sulfate and aluminum concentrations in the stream and in the groundwater resembled those in soil solution. The opposite was true for silica. Compared to earlier samples, catchment runoff silica concentration decreased by 35% on September 15, and by 30% in GW03 groundwater in November. In contrast, DOC concentration in the catchment runoff clearly exceeded the median of throughfall and soil solution concentration.

In the short-term, the increase of electrical conductivity, temperature, and O_2 concentration, and the decrease of pH at GW03 began synchronously with groundwater level increase in mid-September (Figs. 5 and 6). Within 6 h, electrical conductivity and O_2 reached a first maximum and remained fairly constant for 45 or 14 h after the end of rainfall (Fig. 5). Then temperature, electrical conductivity, and O_2 concentration decreased rapidly, and pH increased. A second, much more damped and delayed response was observed, until the groundwater level reached the pre-event level roughly 2 weeks later. A similar pattern of temperature, pH, electrical conductivity, and O_2 was observed in mid-October. In contrast, there was no corresponding response at GW12 (not shown).

5. Discussion

The period described here was selected, because of the clarity of the described phenomena due to the magnitude of rainfall and discharge. Similar observations were made repeatedly during smaller discharge events, since the intensive monitoring program began in 1995.

5.1. Hydrometric data

5.1.1. Groundwater recharge

The saturated hydraulic conductivity of the top soil (see above) exceeds maximum rainfall intensity on September 15 ($7\ mm\ h^{-1}$) by more than two orders of magnitude. Correspondingly, neither overland flow nor any evidence of it, such as litter being washed away or erosion rills was detected outside the saturated areas. In addition, the groundwater level increase of roughly 1 m at GW03 and GW12 corresponds to the rainfall quotient (110 mm between September 14 and 23) over effective porosity (10%).

At most sites, the soil water content increase associated with the transient saturation in the vadoze zone during the mid-September rainstorm was less than 5% (Figs. 2 and 4). In addition, upper soil layer matrix potential started to decrease again, while it continued to increase in the deeper layer. Thus, only a small portion of the total water pool in the vadoze soil was required to propagate the pressure wave down to the water table.

The parallel readings of TDR probes and adjacent tensiometers confirm the translatory flow concept. There is no hint of short-term decoupling of soil water content and soil matrix potential. Assuming Darcian flow, a hydraulic gradient of two would be required for the observed velocity of vertical pressure transmission in the top 35 cm (Table 2). According to the

tensiometer data, the hydraulic gradients in the vadoze zone were between 0.5 and 1.5 during peak discharge on September 15, which is only slightly less.

At a much smaller scale, Göttlein and Manderscheid (1998) observed preferential flow in the top soil of the same watershed. This corresponds with the observation that the effect of preferential flow phenomena often decreases with increasing scale (Torres et al., 1998). It is concluded that at the given scale of observation, hydrometric data are in accordance with the translatory flow concept for groundwater recharge.

5.1.2. Runoff generation

Maximum increase of groundwater level until the end of the September 15 discharge peak was less than 1 m, which is less than 5% of the thickness of the aquifer. Assuming a maximum hydraulic gradient of 0.1, which is roughly equal to mean slope, and the above cited mean hydraulic conductivity of the top soil, the Darcian flow velocity would be in the range of a few cm h^{-1}. It is clear that enhanced groundwater matrix flow accounts only for a negligible portion of the observed 2000% discharge increase coincident with findings from many other sites (Bonell, 1998).

On September 15, the pressure wave reached 0.9 m depth in about half the time lag between precipitation maximum and peak discharge (Table 2). Depth to the water table is even less at many sites in the riparian zone. Due to the softly undulating topography, the soil saturated to the surface in the small depressions first, initiating surface runoff. In addition, part of the runoff might have occurred in the highly porous forest floor layer. This transient network very efficiently drained excess water, as, e.g. even during the most intense precipitation, the water level at the GW04 tensiometers did not exceed about 0.6 m below the surface. Similarly, the increase of groundwater level during rainstorms at the Schlöppnerbrunnen site did not exceed a few cm after the end of August (Fig. 3). Only a small increase of the groundwater level was required to hydraulically connect the riparian zone to the stream and to increase stream discharge. That might explain the discrepancy between the short-term variability of the source area assumed by many runoff models and the apparent constancy of the saturated areas observed in the field (Güntner et al., 1999; Kirnbauer and Haas, 1998).

The more the groundwater level increased at sites further up-slope, the larger the portion of the catchment that was connected hydraulically to the stream during single storms, indicated, e.g. by the Schlöppnerbrunnen data (Figs. 1 and 3). However, the time lag between the maximum rainfall intensity and the corresponding discharge peak (Table 3) depended on neither the antecedent groundwater level nor on rainfall intensity or rainfall amount. This is at odds with the results of Evans et al. (1999), in which the time lag was inversely correlated with precipitation intensity, stream discharge, and runoff coefficient. Perhaps the hourly time resolution of the Lehstenbach data is not sufficient to detect these correlations.

It is remarkable that different studies at different sites yield lag times similar to those in this study (Tables 2 and 3), irrespective of catchment size and total channel length. During an irrigation experiment in an 860 m^2 headwater catchment, Torres et al. (1998) observed a 2.5 h time lag between peak rainfall and peak discharge. Mean lag time for piezometers inside the catchment was 1.7 h in the upper 1 m soil layer, which is only slightly less than that of the Lehstenbach tensiometers at 0.9 m depth. In contrast, mean lag time for runoff at the bedrock surface at approximately 0.5 m depth observed by Buttle and Turcotte (1999) was 0.5–1 h. This is about the same as the lag time observed for tensiometers at 0.35 m depth in the Lehstenbach catchment (Table 2).

Evans et al. (1999) report a mean lag time of 2.8 h for stormflow in the 11.4 km^2 Trout Beck catchment. Güntner et al. (1999) observed time lags of about 2–3 h in the 40 km^2 Brugga watershed. These data are very close to the 2–5 h time lag observed in the 4.2 km^2 Lehstenbach catchment. This suggests that the speed of vertical pressure wave propagation to the shallow groundwater table in the transiently saturated zone determines the rapid response of stream discharge. In contrast, residence time in the channels does not seem to play an important role at that temporal and spatial scale. This is obviously the case in the Lehstenbach catchment (see above).

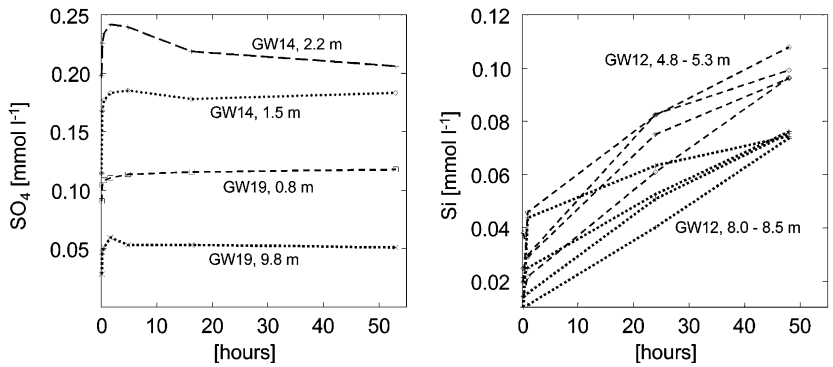

Fig. 9. Kinetics of sulfate desorption (left panel; data: Schweisser, 1998) and silica release (right panel; Rötting, personal communication) of drilling core samples of the Lehstenbach catchment, determined by batch experiments.

5.2. Natural tracer data

5.2.1. Kinetics

Temperature and solute concentration were used as natural tracers. In the short-term, these might be regarded as conservative tracers (Hendershot et al., 1992; Hooper and Shoemaker, 1986; Sidle et al., 2000), depending on the kinetics of the interaction with the soil matrix and with the pre-event water pool.

Time constants of heat transfer in the soil are difficult to quantify at the field scale. At the micro scale, the transfer coefficient depends strongly on the size of the interface between the soil matrix and the liquid face. The nature of the surface plays a crucial role as does the spatial distribution of pre-event and event water. In field studies, temperature data are often interpreted assuming short-term conservative transport in the soil (Kobayashi et al., 1999; Sidle et al., 2000).

The kinetics of geochemical processes depend on a variety of parameters, e.g. the nature of mineral phases, concentrations of competing solutes, etc. (Nielsen et al., 1986). In addition, different processes that are not discussed in this paper determine the interaction between solutes and matrix, e.g. desorption and adsorption, dissolution, precipitation, and diffusion into and out of dead-end pores.

Sulfate desorption kinetics in soil have been quantified in various studies. Based on isotope data in field studies, Mörth and Torsander (1995) conclude that the time constant of sulfate desorption in the field is in the range of minutes. Courchesne and Hendershot (1990) performed batch experiments with soil samples from two Canadian podzols and found that 50% of the totally desorbed SO_4 was desorbed within the first 5 min. Alewell (1998) performed desorption experiments with top soil samples from the Lehstenbach watershed and two other sites. Desorbed sulfate from undisturbed soil columns sprinkled with 10 mm day^{-1} differed only slightly from that desorbed in batch experiments shaken for 18 h. Schweisser (1998) studied drilling core samples from up to 10 m depth in the Lehstenbach catchment. After a 10 min shaking interval, solution sulfate concentration exhibited about 85–88% of that measured after 7 days (Fig. 9). In two of the samples, sulfate concentration slightly decreased after 4 days, which might be due to precipitation.

The kinetics of silica dissolution is often assumed to be rather slow. Hooper and Shoemaker (1986) compared results of hydrograph separation by deuterium and silica and described similar results. Simonsson and Berggren (1998) performed batch experiments with soil samples from the B horizon of different Swedish podzols with 1 mM NaCl or 2 mM HCl. They found a clear and nearly linear increase in silica concentration with time up to 27 days in three out of four samples. In contrast, Wels et al. (1991) observed rapid equilibration of soil water with silica of the soil matrix within a few hours, both in the field and in the laboratory. However, different soil types varied considerably with respect to their silica kinetics. In a preliminary study, samples from Lehstenbach catchment drilling cores were investigated. The samples were shaken with solutions similar to mean groundwater concentration, but without silica

and with varying ionic strength (Rötting, unpublished data). Although the rate of silica concentration increase was the highest in the first 10 min, silica concentration of the solution continued to increase for 48 h until the end of the experiment (Fig. 9). The results are similar to those of Simonsson and Berggren (1998). Despite the limited number of replicates, the data clearly suggest that the silica kinetics in the Lehstenbach is considerably slower than that of sulfate.

In addition to silica dynamics, Simonsson and Berggren (1998) investigated, in the same samples, the kinetics of quickly reacting aluminum. In contrast to silica, aluminum concentration was highest in the first (0.2 days) or second step (5 days) of the batch experiments. Franken et al. (1995) studied the aluminum kinetics of undisturbed soil samples from the A and B horizons of the Lehstenbach catchment. Undersaturation of Al could not be detected for steady state flow with 4 and 12 mm day^{-1}, but was obvious for 36 mm day^{-1}. The maximum daily rainfall was 7 mm h^{-1} on September 15, 1998. Related to the respective pore volume, the aluminum free signal of throughfall would be entirely buffered between 0.9 and 2.8 m depth.

5.2.2. Observed tracer dynamics

Despite its higher groundwater level, groundwater solute concentration and groundwater level response at GW12 was less pronounced than in GW03. This can be attributed to the clayey layers at 0.8–2.2 m depth at GW12. The probe at GW12 was installed 7.2 m below the groundwater level, in contrast to 4.4 m at GW03 (see earlier).

During the heavy rainstorms, sulfate and aluminum concentrations in groundwater recharge at GW03 (Fig. 8) and stream discharge (Fig. 7) exhibited a shift toward pre-event water concentrations in the vadoze zone instead of toward event water, i.e. throughfall. The change of solute concentration in GW03 groundwater is evidently due to exchange in the overlying soil layers and not due to local equilibrium in the layer that becomes additionally saturated, since the hydrochemical parameters returned to the pre-event level much earlier than the groundwater level (Fig. 5). In addition, the change of solute concentration exceeds the median gradient of solute concentration over depth determined by Rötting (2000) by more than one order of magnitude. Thus, the sulfate and aluminum data at the given scale of observations are in accordance with the translatory flow concept. The same holds for temperature data during groundwater recharge (Fig. 6).

However, conservative mixing of pre-event and event water in the vadoze zone also needs to be considered. Sidle et al. (2000) conclude from soil and discharge temperature data that rapid mixing takes place in the vadoze zone even during stormflow. Experimental data from Jardine et al. (1990) and Brandi-Dohrn et al. (1996) show that the vertical transport velocity of a bromide tracer in the large pores of the subsoil exceeds that of the small pores by far, but the difference diminishes with increasing depth, indicating increasing mixing between small pore and large pore water. The concept can also be extended to the catchment scale. The fractal filtering of the chloride input signal that was observed at various catchments could be traced back to advection and dispersion of spatially distributed rainfall inputs along flowpaths of different lengths (Kirchner et al., 2000, 2001).

Obviously, mixing of throughfall and soil solution during groundwater recharge was restricted to a small fraction of the total soil water volume. The total amount of precipitation from September 20 to October 14 was 100 mm. The size of the pre-event water pool in the overlying 3 m thick vadoze zone, assuming a rather low water content of 30% (Fig. 4), is about 900 mm. Assuming further that throughfall silica concentration is zero, conservative mixing would result in at most a 10% decrease of silica concentration in the vadoze zone. In contrast, the observed 16% decrease in groundwater silica concentration at GW03 between September 7 and October 14 is likely to be a substantial underestimation of silica concentration of the recharging water due to the depth-integrating sampling procedure (see above).

Thus, the silica data provide strong evidence that a substantial fraction of event water reaches deeper layers during the major rainstorms, bypassing the largest fraction of the soil water store. In contrast to sulfate and aluminum, only the silica kinetics is sufficiently slow to kinetically constrain the solute turnover and to clearly show that effect. Based on deuterium data, Stewart and McDonnell (1991) found evidence for small-scale preferential flow and subsequent mixing with the soil water pool. Similarly,

Landon et al. (2000) found a hybrid model that combined small-scale piston-flow displacement and subsequent mixing to be the most adequate for modeling the observed stable isotope dynamics. Leaney et al. (1993) state that the observed dampening of the rainfall isotope signal is due to mixing with pre-event water within the macropores. In addition, Robson et al. (1993) conclude that the apparent constancy of stream solute concentration during stormflow in a low order catchment is due to the very rapid kinetics of solute exchange.

Silica data in the catchment runoff confirm that conclusion. Assuming deep groundwater contribution to be constant and equal to pre-event baseflow, and conservative mixing of throughfall and top soil solution each with median pre-event solute concentration, throughfall would account for about 37% of peak discharge according to the silica data. This is likely to underestimate the event water contribution due to coarse temporal resolution (daily composite sample) in the stream data. Substantial changes of silica concentration in stream water are observed at the scale of hours rather than days even in substantially larger basins (Lischeid and Uhlenbrook, 2002).

DOC concentration in catchment runoff during discharge peaks exceeded the median concentration of soil solution at 20–200 cm depth (Fig. 7, Table 4). Hornberger et al. (1994) modeled the DOC dynamics in the runoff of a small forested catchment assuming mobilization in the top soil layer of the riparian zone. Likewise, Hagedorn et al. (2000) identified the near-stream top soil layer to be the dominating DOC source during stormflow in a small Swiss catchment, based on a hydrograph analysis for the different fractions of DOC.

This points to the influence of the riparian zone on stormflow stream water chemistry. The Lehstenbach hydrometric data indicate that discharge peaks were generated by excess water that ran off on the surface or through the forest floor of the riparian zone. However, despite minimal contact time with the soil matrix, sulfate and aluminum concentrations are similar to pre-event soil water (Fig. 7, Table 4). Waddington et al. (1993), and Brassard et al. (2000) trace this apparent discrepancy to rapid mixing of infiltrating throughfall with a considerable store of pre-event water in the vadoze zone, due to turbulent flow and the kinetic energy of raindrops falling on the water surface. The different behavior of sulfate, aluminum, and silica in the Lehstenbach watershed shows that short-term exchange with the matrix also plays an important role.

6. Conclusions

Groundwater and stream water contamination risk assessment depends on a sound understanding of short-term hydrological dynamics. The Lehstenbach study combined comprehensive hydrometric and hydrochemical measurements to enhance understanding of these short-term stream discharge and groundwater recharge dynamics.

The results show that the scale of observation and the observed parameters determine the extent to which water flow can be described as translatory or preferential flow. Tensiometer and TDR readings in the vadoze zone indicate a rapid propagation of the wetting front down to the groundwater level at 3 m depth. The data do not provide any evidence for preferential flow and the dynamics can be described as transient flow. Stormflow generation was restricted to surface or near-surface runoff in the riparian zone. In contrast to the common assumption of a highly dynamic horizontal extension of the saturated area influencing storm runoff, minor changes of the groundwater level in the riparian zone determined the rapid increase of discharge from the Lehstenbach catchment.

Temperature, sulfate, aluminum, and DOC dynamics during groundwater recharge and stormflow generation can be described as translatory flow. However, the silica data elucidate the role of solute exchange with the soil matrix. The infiltrated event water reached the groundwater table up to a depth of 3 m, bypassing the largest part of the soil water store. A few hours' contact time with the soil matrix was sufficient to allow sulfate and aluminum equilibration with the matrix, but not silica, due to the slow kinetics of silica dissolution. This holds for saturated area runoff as well, because of the small-scale pattern of groundwater recharge and return flow in the riparian zone. These results emphasize that preferential flow phenomena are not so much

due to inherent properties of the soil matrix as depending on the scale of observation and the observed parameters and their kinetics of equilibrating with the matrix during subsurface transport.

Due to rapid equilibration with the soil matrix, stream water concentration of, e.g. sulfate, during discharge peaks can be used as a spatial integral for monitoring mid-term changes in the top soil. This would allow researchers to circumvent some of the difficulties of the enormous spatial heterogeneity of soil solution encountered in the field (Neal et al., 1997; Manderscheid and Matzner, 1995). The potential of this approach has been demonstrated by an analysis of the Lehstenbach sulfate concentration data to investigate the effects of decreasing sulfur deposition on soil water, groundwater, and stream water quality (Lischeid, 2001).

Acknowledgments

The authors would like to thank Klaus Moritz and Jochen Bittersohl from the Bavarian State Office for Water Management for data and discussion. Thanks to the crew of the central lab of BITÖK that processed hundreds of samples, and to Jörg Gerchau and Otto Klemm from the Department of Climatology of BITÖK for the meteorology data. The help of Uwe Hell in performing field work under rugged conditions is highly appreciated. This work was funded by the German Federal Ministry for Education, Science, Research and Technology (BMBF) under grant no. 0339476 C. Last but not least, Kendall Watkins helped to improve the English text.

References

Alewell, C., 1998. Investigating sulfate sorption and desorption of acid forest soils with special consideration of soil structure. Z. Pflanzenernähr. Bodenk. 161, 73–80.

Anderson, S.P., Dietrich, W.E., Torres, R., Montgomery, D.R., Loague, K., 1997. Concentration–discharge relationships in runoff from a steep, unchanneled catchment. Water Resour. Res. 33, 211–225.

Beven, K., 2001a. On hypothesis testing in hydrology. Hydrol. Process. 15, 1655–1657.

Beven, K., 2001b. How far can we go in distributed modelling? Hydrol. Earth Syst. Sci. 5, 1–12.

Beven, K., German, P., 1982. Macropores and water flow in soils. Water Resour. Res. 18, 1311–1325.

Bonell, M., 1998. Selected challenges in runoff generation research in forests from the hillslope to headwater drainage basin scale. J. Am. Water Resour. Assoc. 34, 765–785.

Brandi-Dohrn, F.M., Dick, R.P., Hess, M., Selker, J.S., 1996. Suction cup sampler bias in leaching characterization of an undisturbed field soil. Water Resour. Res. 32, 1173–1182.

Brassard, P., Waddington, J.M., Hill, A.R., Roulet, N.T., 2000. Modelling groundwater–surface water mixing in a headwater wetland: implications for hydrograph separation. Hydrol. Process. 14, 2697–2710.

Burns, D.A., Hooper, R.P., McDonnell, J.J., Freer, J.E., Kendall, C., Beven, K., 1998. Base cation concentrations in subsurface flow from a forested hillslope: the role of flushing frequency. Water Resour. Res. 34, 3535–3544.

Buttle, J.M., Turcotte, D.S., 1999. Runoff processes on a forested slope on the Canadian Shield. Nordic Hydrol. 30, 1–20.

Courchesne, F., Hendershot, W.H., 1990. Kinetics of sulfate desorption from two spodosols of the Laurentians. Quebec. Soil Sci. 150, 858–866.

Evans, M.G., Burt, T.P., Holden, J., Adamson, J.K., 1999. Runoff generation and water table fluctuations in blanket peat: evidence from UK data spanning the dry summer of 1995. J. Hydrol. 221, 141–160.

Flühler, H., Durner, W., Flury, M., 1996. Lateral solute mixing processes. A key for understanding field-scale transport of water and solutes. Geoderma 70, 165–183.

Franken, G., Pijpers, M., Matzner, E., 1995. Al chemistry of the soil solution in an acid forest soil as influenced by percolation rate and soil structure. Eur. J. Soil Sci. 46, 613–619.

Gerke, H.H., van Genuchten, M.Th., 1993. A dual-porosity model for simulating the preferential movement of water and solutes in structured porous media. Water Resour. Res. 29, 305–319.

Goodrich, D.C., Woolisher, D.A., 1991. Catchment hydrology. Rev. Geophys. Supplement, 202–209.

Göttlein, A., Manderscheid, B., 1998. Spatial heterogeneity and temporal dynamics of soil water tension in a mature Norway spruce stand. Hydrol. Process. 12, 417–428.

Güntner, A., Uhlenbrook, S., Seibert, J., Leibundgut, Ch., 1999. Multi-criterial validation of TOPMODEL in a mountainous catchment. Hydrol. Process. 13, 1603–1620.

Hagedorn, F., Schleppi, P., Waldner, P., Flühler, H., 2000. Export of dissolved organic carbon and nitrogen from Gleysol dominated catchments—the significance of water flow paths. Biogeogemistry 50, 137–161.

Hauck, A., 1999. Hydrogeologische Charkterisierung des Lehstenbach-Einzugsgebietes am Großen Waldstein—Messung und Simulation. Diploma Thesis, University of Bayreuth (in German).

Hendershot, W.H., Savoie, S., Courchesne, F., 1992. Simulation of stream-water chemistry with soil solution and groundwater flow contributions. J. Hydrol. 136, 237–252.

Hooper, R.P., Shoemaker, C.A., 1986. A comparison of chemical

and isotopic hydrograph separation. Water Resour. Res. 22, 1444–1454.

Hornberger, G.M., Bencala, K.E., McKnight, D.M., 1994. Hydrological controls on dissolved organic carbon during snowmelt in the Snake River near Montezuma, Colorado. Biogeochemistry 25, 147–165.

Jardine, P.M., Wilson, G.V., Luxmoore, R.J., 1990. Unsaturated solute transport through a forest soil during rain storm events. Geoderma 46, 103–118.

Jones, J.A.A., 1987. The effects of soil piping on contributing areas and erosion patterns. Earth Surf. Process. Landforms 12, 229–248.

Kirkby, M., 1988. Hillslope runoff processes and models. J. Hydrol. 100, 315–339.

Kirnbauer, R., Haas, P., 1998. Observations on runoff generation mechanisms in small Alpine catchments. IAHS Publ. 248, 239–247.

Kirchner, J.W., Xiahong, F., Neal, C., 2000. Fractal stream chemistry and its implications for contaminant transport in catchments. Nature 403, 524–527.

Kirchner, J.W., Xiahong, F., Neal, C., 2001. Catchment-scale advection and dispersion as a mechanism for fractal scaling in stream tracer concentrations. J. Hydrol. 254, 82–100.

Kobayashi, D., Ishii, Y., Kodama, Y., 1999. Stream temperature, specific conductance and runoff process in mountain watersheds. Hydrol. Process. 13, 865–876.

Landon, M.K., Delin, G.N., Komor, S.C., Regan, C.P., 2000. Relation of pathways and transit times of recharge water to nitrate concentrations using stable isotopes. Ground Water 38, 381–395.

Lange, H., Lischeid, G., Hauhs, M., 1995. Shallow water flow in a deeply weathered granite aquifer and implications for hydrochemical models. Water, Air Soil Pollut. 85, 1825–1830.

Leaney, F.W., Smettem, K.R.J., Chittleborough, D.J., 1993. Estimating the contribution of preferential flow to subsurface runoff from a hillslope using deuterium and chloride. J. Hydrol. 147, 83–103.

Lischeid, G., 2001. Investigating short-term dynamics and long-term trends of SO_4 in the runoff of a forested catchment using artificial neural networks. J. Hydrol. 243, 31–42.

Lischeid, G., Uhlenbrook, S., 2002. Checking a process-based catchment model by artificial neural networks. Hydrol. Process. in press.

Luxmoore, R.J., Jardine, P.M., Wilson, G.V., Jones, J.R., Zelazny, L.W., 1990. Physical and chemical controls of preferred path flow through a forested hillslope. Geoderma 46, 139–154.

Manderscheid, B., Matzner, E., 1995. Spatial heterogeneity of soil solution chemistry in a mature Norway Spruce (Picea abies (L.) Karst.) Stand. Water, Air, Soil Pollut. 85, 1185–1190.

Matzner, E., Alewell, C., Bittersohl, J., Lischeid, G., Kammerer, G., Manderscheid, B., Matschonat, G., Moritz, K., Tenhunen, J.D., Totsche, K., 2001. Biogeochemistry of a spruce forest catchment of the Fichtelgebirge in response to changing atmospheric deposition. In: Tenhunen, J.D., Lenz, R., Hantschel, R. (Eds.), Ecosystem Approaches to Landscape Management in Central Europe, Ecological Studies, vol. 147. Springer, Heidelberg, pp. 463–504.

McDonnell, J.J., 1990. A rationale for old water discharge through macropores in a steep, humid catchment. Water Resour. Res. 26, 2821–2832.

Moritz, K., Bittersohl, J., Müller, F.X., Krebs, M., 1994. Auswirkungen des Sauren Regens und des Waldsterbens auf das Grundwasser—Methoden und Daten des Entwicklungsvorhabens 1988–1992. Bayerisches Landesamt für Wasserwirtschaft, München, Materialien Nr. 40 (in German).

Mörth, C.-M., Torsander, P., 1995. Sulfur and oxygen isotope ratios in sulfate during an acidification reversal study at Lake Gardsjön, Western Sweden. Water, Air, Soil Pollut. 79, 261–278.

Neal, C., Hill, T., Hill, S., Reynolds, B., 1997. Acid neutralization capacity measurements in surface and groundwaters in the Upper River Severn, Plynlimon: from hydrograph splitting to water flow pathways. Hydrol. Earth Syst. Sci. 3, 687–696.

Nielsen, D.R., van Genuchten, M.Th., Biggar, J.W., 1986. Water flow and solute transport processes in the unsaturated zone. Water Resour. Res. 22, 89S–108S.

Noguchi, S., Tsuboyama, Y., Sidle, R.C., Hosoda, I., 1999. Morphological characteristics of macropores and the distribution of preferential flow pathways in a forested slope segment. Soil Sci. Soc. Am. J. 63, 1413–1423.

Rawlins, B.G., Baird, A.J., Trudgill, S.T., Hornung, M., 1997. Absence of preferential flow in the percolating waters of a coniferous forest soil. Hydrol. Process. 11, 575–585.

Rice, K.C., Hornberger, G.M., 1998. Comparison of hydrochemical tracers to estimate source contributions to peak flow in a small, forested, headwater catchment. Water Resour. Res. 34, 1755–1766.

Robson, A.J., Neal, C., Hill, S., Smith, C.J., 1993. Linking variations in short- and medium-term stream chemistry to rainfall inputs—some observations at Plynlimon. Mid-Wales. J. Hydrol. 144, 291–310.

Rötting, T., 2000. Entwicklung einer Methode der tiefenorientierten Grundwasserbeprobung in durchgehend verfilterten Brunnen. Diploma Thesis, University of Bayreuth (in German).

Sager, H., Bittersohl, J., Haarhoff, T., Haberger, I., Moritz, K., 1990. Fate of atmospheric deposition in small catchments depending on local factors. Hydrology in Mountainous Regions. I. Hydrological Measurements; the Water Cycle. Proceedings of two Lausanne Symposia, August 1990, IAHS Publ. 193, pp. 733–740.

Schweisser, T., 1998. Sulfatsorptions- und -desorptionsverhalten des oberflächennahen, geologischen Untergrundes im Wassereinzugsgebiet Lehstenbach (Fichtelgebirge). Diploma Thesis, University of Bayreuth (in German).

Sidle, R.C., Tsuboyama, Y., Noguchi, S., Hosoda, I., Fujieda, M., Shimizu, T., 2000. Stormflow generation in steep forested headwaters: a linked hydrogeomorphic paradigm. Hydrol. Process. 14, 369–385.

Simonsson, M., Berggren, D., 1998. Aluminium solubility related to secondary solid phases in upper B horizons with spodic characteristics. Eur. J. Soil Sci. 49, 317–326.

Stewart, M.K., McDonnell, J.J., 1991. Modeling base flow soil water residence times from deuterium concentrations. Water Resour. Res. 27, 2681–2693.

Torres, R., Dietrich, W.E., Montgomery, D.R., Anderson, S.P., Loague, K., 1998. Unsaturated zone processes and the hydrologic response of a steep, unchanneled catchment. Water Res. Resour. 34, 1865–1879.

Waddington, J.M., Roulet, N.T., Hill, A.R., 1993. Runoff mechanisms in a forested groundwater discharge wetland. J. Hydrol. 147, 37–60.

Wels, C., Cornett, R.J., Lazerte, B.D., 1991. Hydrograph separation: a comparison of geochemical and isotope tracers. J. Hydrol. 11, 253–274.

Zoller, U., Goldenberg, L.C., Melloul, A.J., 1998. The short-cut enhanced contamination of the Gaza Strip coastal aquifer. Water Res. 32, 1179–1788.